12TH ASIA-PACIFIC CONFERENCE ON COMBUSTION (ASPACC 2019)

1-5 JULY, 2019

FUKUOKA, JAPAN

SECOND CIRCULAR

Photo: Fukuoka City

The Asia-Pacific Conference on Combustion (ASPACC) is a biennial meeting sponsored by the Combustion Institute and organized by members of the Asia-Pacific regional sections. Its goal is to promote exchange of information and to elevate combustion science and technology through regional and global scientific partnership. The 12th ASPACC will be hosted by the Japan Section of the Combustion Institute, and will be held on July 1 to 5, 2019 in Fukuoka, Japan. The conferences will provide a forum for mutual exchange of information in the Asia-Pacific combustion community involved in both fundamental and application oriented research and development works.

PLENARY SPEAKERS :

Professor Evatt Hawkes, University of New South Wales
Unravelling engine combustion using large-scale computations

Professor Naian Liu, University of Science and Technology of China
Combustion of Fire Whirl : How much do we know?

Professor Kang Y. Huh, Pohang University of Science and Technology
Combustion Modeling and Simulation in Era of the Fourth Industrial Revolution

Professor Min Suk Cha, King Abdullah University of Science and Technology
Recent understanding with flames under external electric fields

Professor Yei-Chin Chao, National Cheng Kung University
Hydrogen Peroxide Revisited : the Role as an Energy-Saving Combusiton Enhancer and a Non-Toxic Green Propellant for Satellites and Hybrid Rockets

Speakers from Japan and India Sections are to be determined.

CONFERENCE VENUE :

Fukuoka International Congress Center
2-1 Sekijo-machi, Hakata-ku, Fukuoka 812-0032, JAPAN

IMPORTANT DATES :

Submission of full paper:	25th January 2019
Notification of paper acceptance:	1st April 2019
Conference dates:	1st - 5th July 2019

PAPER SUBMISSION :

Full length papers should follow the format given on the conference web site. The Program Committee will select papers for presentation on the basis of peer reviews of each paper. All selected papers should be presented by one of the authors. Technical papers are solicited in all areas of combustion science and technology including the following areas.

- Gas-Phase Reaction Kinetics
- Soot, Nanomaterials, and Large Molecules
- Diagnostics
- Laminar Flames
- Turbulent Flames
- Spray, Droplet, and Supercritical Combustion
- Detonations, Explosions, and Supersonic Combustion
- Solid Fuel Combustion
- Fire Research
- Stationary Combustion System and Control of Greenhouse Gas Emissions
- Internal Combustion Engines
- Gas Turbine and Rocket Engine Combustion
- New Concepts

YOUNG INVESTIGATOR AWARDS :

Young Investigator Awards will be awarded to the best performing young author-presenter from research students or postdoctoral researchers (or equivalent).

BEST PAPER AWARDS :

Best paper awards will be awareded to the best papers presented at ASPACC2019.

WOMEN IN COMBUSTION MEETING :

All women conference participants are invited to join together for a time to network and share their experiences. The interactive meeting will convene during the conference.

ORGANIZING COMMITTEE :

Chair: Toshiaki Kitagawa, Kyushu University
Co-chair: Fumiteru Akamatsu, Osaka University
Co-chair: Kenji Yamamoto, Mitsubishi Heavy Industries, Ltd.
In 2019, the Organizing Committee is spread in the community of the Asia-Pacific regional sections of the Combustion Institute, mainly the Japan Section.

PROGRAM COMMITTEE :

Chair: Masato Mikami, Yamaguchi University
Co-chair: Shuhei Takahashi, Gifu University

CONTACT :

For additional information please contact
Contact address: aspacc19@combustionsociety.jp
Website: http://www.combustionsociety.jp/aspacc19/

Full length paper submission will be available in early December on the conference web.

Room 5 (411/412)

OS8-13. Solid Fuel Combustion

Fri., 5 Jul., 09:30 - 10:50, Room 5 (411/412)

Chair: **Jian Gao** (Qingdao Institute of Bioenergy and Bioprocess Technology, Chinese Academy of Sciences, China)

ASPACC2019-1243	**Short-Wave Emission Spectrum Features During Fast High-Temperature Reactions of Condensed Systems** Alexander Ivanovich Kirdyashkin (Far Eastern Federal University, Russian Federation), Ramil Mahmutovich Gabbasov (Tomsk Scientific Center SB RAS, Russian Federation), Vitaly Georgievich Salamatov (Merzhanov Institute of Structural Macrokinetics and Materials Science RAS, Russian Federation), Aleksey Nikolaevich Panchenko (Institute of High Current Electronics SB RAS, Russian Federation), Sergey Sergeevich Minaiv (Far Eastern Federal University, Russian Federation)
ASPACC2019-1248	**The adverse effects of moisture on the natural aging of zirconium-based energetic material** Byungheon Han (Seoul National University, Korea, Korea), Kanagaraj Gnanaprakash (Seoul National University, Korea), Jack J Yoh (Seoul National University, Korea, Korea)
ASPACC2019-1340	**Slow and fast thermal decomposition characteristics of metalized explosives in fuel-rich and oxygen-rich conditions** Yoonsik Park, Yoocheon Kim, Jack J Yoh (Seoul National University, Korea)

12th Asia-Pacific Conference on Combustion,
Fukuoka International Congress Center, Fukuoka, Japan
1st -5th July 2019.

Slow and fast thermal decomposition characteristics of metalized explosives in fuel-rich and oxygen-rich conditions

Yoonsik Park[1], **Yoocheon Kim**[1], **Jack J Yoh**[1*]

[1] Department of Mechanical & Aerospace Engineering, Seoul National University

1 Gwanakro, Gwanakgu, Seoul, 151-742, Republic of Korea

Abstract

The thermal decomposition characteristics of polymer-bonded explosive (PBX) including powdered metal fuel and inorganic oxidizer are analyzed and the relevant chemical kinetics are extracted. The goal is to propose the methodology for simulating the slow and fast cook-off phenomenon. Differential scanning calorimetry (DSC) is performed to define the decomposition characteristics while isoconversional technique is used to construct the relevant reaction model. In particular, to establish the order in which RDX and AP play in reacting sequence, Scanning Electron Microscope and Energy Dispersive Spectroscopy (SEM-EDS) are used to confirm the kinetic model proposed. The slow and fast cook-off simulation is performed, and the relevant runaway characteristics are validated against the experimental measurements.

1 Introduction

All papers Polymer-bonded explosive (PBX) is produced by mixing additives according to various operating purposes based on oxidizing agents such as cyclotetramethylene-tetranitramine (HMX) or cyclotrimethylene-trinitramine (RDX). Usually, when metal fuels are added, effectively total heat of reaction increases together with its impulse amount [1]. In addition, adding more oxidizer such ammonium perchlorate (AP) to PBX may significantly enhance the intended after burning characteristics. Such multifunctional aspect of metalized explosives is typically observed when the shock-induced detonation occurs and subsequent burning of metal powders takes place. However, when thermally heated, these types of explosives are subject to thermal decomposition that develops into a thermal runaway or so called thermal cook off. Therefore, a lot of studies recently aims to understand the thermally induced reaction characteristics of PBX composed of metallic powders and additional oxidizer such as AP, and to construct the appropriate chemical kinetic models for simulating both slow and fast cook-off experiments for model validation.

In this study, we designed three types of samples that are pristine (no metal) PBX (95% HMX with a binder), metallized HMX (66% HMX and 25% Al with binder), and metallized RDX with extra oxidizer (20% RDX, 25% Al, and 43% AP). The kinetics of three PBXs is extracted using DSC. In particular, the third sample has been looked at microscopically via SEM and EDS to identify the complex or multiple reaction sequence due to the addition of AP. Here, SEM is used to identify the overall shape of the sample, and EDS is utilized for the composition analysis [2]. The cook off simulations in both low heating and fast heating rates are conducted by using the obtained chemical kinetics. Also, the corresponding cook-off experimental measurements were made available for validating the numerical prediction of time and temperature at which thermal runaway occurred.

2 DSC experiment

2.1 Experimental method

DSC experiments are carried out with a Mettler Toledo DSC 3 instrument utilizing the HP reusable sealed crucible 30 µL for first and second samples and standard 40 µL sealed aluminum pans for third sample. The experiments are conducted with a purge flow of nitrogen maintained at 80 mL min^{-1}. The sealed pans allow observation of the decomposition process without detrimental effect of energetic material evaporation. For all DSC signals, positive going feature corresponds to exothermic process. The PBX samples are tested under non-isothermal experimental conditions without self-heating phenomenon [3].

2.1 Experimental result

The activation energy and pre-exponential factor varying with λ are shown in Fig. 1. This implies that the extracted kinetics describes the complete process of the chemical reaction through a set of Arrhenius parameters obtained at an instantaneous state of the reaction progress. The heat of reaction for each samples are shown in Table. 1.

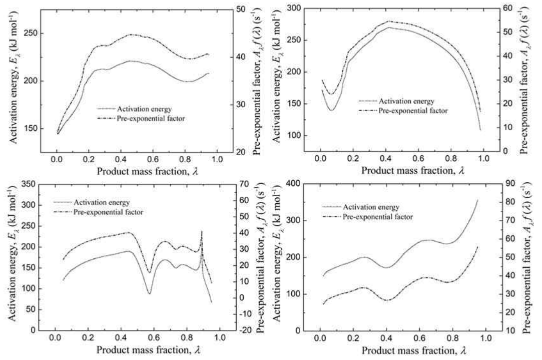

Figure 1: Activation energy and pre-exponential factor parametrized by the progress of reaction λ. (Clockwise from top left, PBX #1, #2, AP of #3 and RDX of #3)

Corresponding author. Fax: +82-02-880-1507
E-mail address: jjyoh@snu.ac.kr

Heat of reaction (J/g)	Sample#1 95%HMX	Sample#2 66%HMX	Sample #3 25% RDX 30% AP	
	1940.32	1279.56	380.54	1270.5

Table 1: Heat of reactions for tested PBX samples. Al reacts at above 2000 °C and thus heat of reaction values do not include contribution from Al in each sample.

3 SEM-EDS result

In the current study, we assumed that the RDX first start the decomposition/exothermic reaction and then the AP sequentially initiates the decomposition/exothermic reaction in the process of establishing the kinetics of PBX #3 in Section 2. To confirm the validity of these assumptions, verification experiments are performed using DSC and SEM-EDS. The experimental method is as follows. First, as shown in Fig. 2, the DSC experiment is carried out at 15 °C/min heating rate for PBX #3. And it set the A, B and C points according to temperature range. Point A represents the raw material state of PBX #3 and point B represents the point just after the RDX decomposition/exothermic reaction of PBX #3 is terminated and the decomposition/exothermic reaction of AP begins. Point C indicates the region at which the decomposition/exothermic reaction of the AP is terminated. The PBX #3 sample is recovered by reopening the DSC crucible after the DSC experiment is completed at each point of A, B, and C.

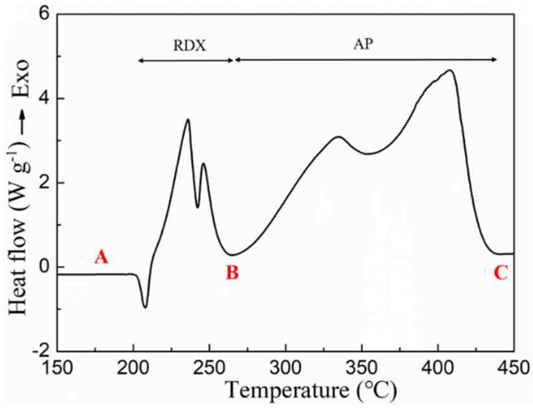

Figure 2: Sample extraction point for A, B and C from DSC at heating rate of 15 °C/min

SEM-EDS experiments are performed to analyze the composition of A, B and C samples. SEM images of A, B and C samples are shown in Fig. 3 and EDS composition analysis results are shown in Table 2. The EDS analysis is performed for the entire area shown in Fig. 3. Before looking at the results of the EDS, chemical formula of RDX and AP are $C_3H_6N_6O_6$ and NH_4ClO_4, respectively. First, in order to investigate the reaction of RDX by EDS analysis, a comparison of the composition between the sample A and the sample B, it can be identified by comparing the composition of the carbon which is not contained in the AP. And to investigate the reaction of AP, it can be confirmed by comparing the composition of chlorine between sample B and C, which is not included in RDX and binder components. Binder used in PBX #3 is HTPB and DOA which composed of Carbon, Hydrogen, and Oxygen.

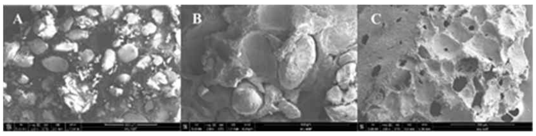

Figure 3: SEM images of samples A, B, and C

From the EDS results of sample C, it is clear that the reaction of RDX and AP is completed at sample C, so that the composition of the background carbon by the binder is confirmed as ~31%. Based on this, the composition of the sample A and the sample B is compared. The carbon composition of sample B is 31.07%, which is consistent with the carbon composition of the binder. The carbon composition of sample A which RDX is contained is 37.36%. From this, it can be confirmed that the carbon contained in RDX has disappeared by the decomposition reaction of RDX. For comparison of sample B and sample C, it can be observed that the composition of chlorine and nitrogen, which are not contained in binder but contained only in AP, are remarkably decreased or very small fraction is measured. From these results, we can confirm that RDX is decomposed in A to B process and AP is decomposed in B to C process.

SEM images of Fig. 3 show this chemical reaction process visually. A comparison of the SEM images of samples A and B reveals that the polygon-shaped RDX crystal disintegrates and disappears and the PBX is punctured. Comparing the SEM images of samples B and C, we can see that the crystals of the AP disappear and only the binder and aluminum particles remain entangled.

Weight %			
	A	B	C
C	37.36	31.07	31.23
N	17.85	14.28	3.02
O	24.41	26.10	2.61
Al	10.29	15.04	62.94
Cl	10.09	13.51	0.2

Table 2: EDS analysis for composition of sample A, B and C

4 Two types of thermal cook-off tests: slow and fast

4.1 Slow cook-off

To show validity and applicability of the extracted kinetics, we conduct the simulation of the slow cook-off test. And actual slow cook off test also have been conducted. The governing equations are as follows:

$$\rho C\frac{\partial T}{\partial t}=k\left(\frac{\partial^2 T}{\partial x^2}+\frac{\partial^2 T}{\partial y^2}\right)-\frac{\partial \lambda}{\partial t}Q \tag{1}$$

$$\frac{d\lambda}{dt}=A_\lambda f(\lambda)\exp\left(\frac{-E_\lambda}{RT}\right) \tag{2}$$

ρ , C and k are density, specific heat and thermal conductivity respectively for PBXs. Values for PBXs are summarized in table 3. Equation (1) is the energy conservation. To describe the heating process, heat conduction is included in two-dimensional spatial domain. In this experiment, the energetic materials do not ‘flow’ during the constant heating process. Thus mass and momentum are unchanged. The kinetic parameters shown in Fig. 1 is used in solving the reaction progress in Eq. (2). The second-order central difference is used for the spatial discretization, and a third-order Runge-Kutta method is used for time integration.

	PBX #1	PBX #2	PBX #3
ρ (kg/m^3)	1820	1900	1820
C (J/kg·K)	1180.4	1096.3	1079.8
k (W/m·K)	0.385	0.997	0.201

Table 3: Density, specific heat and thermal conductivity for PBXs

The slow cook-off test is a standardized experiment for monitoring the violence of reaction of insensitive munitions [4]. The obtained measurements from the test are the time and temperature until the thermal runaway and the classification of the reaction being mild as deflagration to as severe as detonation.

The material of casing is a steel with its density of 7870 kg/m^3. Its thermal conductivity is 49.56 W/m·K and the specific heat is 474.98 J/kg·K. The material properties of steel are referred from [5]. The inside of cylindrical case is filled with the PBX. The temperature of the charge is measured at the center. The thickness of the case is 0.4 cm. The width and length of the charge are 4.5 cm and 20.0 cm, respectively. The initial temperature of PBX is 30.8 °C and then it is heated to 108 °C within 1 hour. The heater temperature is maintained at 108 °C for 7 hours to allow temperature to equilibrate before the final runaway is allowed to occur. Then the heating rate of 3.3 °C/hour is used until explosion is witnessed.

The corresponding explosion time and temperature are summarized in Table 4. For PBX #1, the values reported in the literature for LX-10 explosives of the same composition with 95% HMX are used for this comparison [6]. A very good agreement between the experiment and simulation is observed.

4.2 Fast cook-off

4.2.1 Numerical set up

The calculation and experiment results are compared using the kinetics with feasibility at low heating rates. The governing equations used in fast cook off simulation are as follows:

For explosives

$$\frac{\partial \vec{U}}{\partial t}+\frac{\partial \vec{E}}{\partial r}+\frac{\partial \vec{F}}{\partial z}=\vec{S}\left(\vec{U}\right) \tag{3}$$

$$\vec{U}=\begin{bmatrix}\rho\\ \rho u\\ \rho v\\ \rho E\\ \rho\lambda_{exp}\end{bmatrix}\ \vec{E}=\begin{bmatrix}\rho u\\ \rho u^2+p\\ \rho uv\\ u(\rho E+p)\\ \rho\lambda_{exp}u\end{bmatrix}\ \vec{F}=\begin{bmatrix}\rho v\\ \rho vu\\ \rho v^2+p\\ \mathrm{v}(\rho E+p)\\ \rho\lambda_{exp}v\end{bmatrix}\ \vec{S}=\begin{bmatrix}0\\ 0\\ 0\\ k\nabla^2T+\rho Q\,\dot{\lambda}_{\mathrm{exp}}\\ \rho\,\dot{\lambda}_{exp}\end{bmatrix}$$

For steel container

$$\frac{\partial \vec{U}}{\partial t}+\frac{\partial \vec{E}}{\partial r}+\frac{\partial \vec{F}}{\partial z}=\vec{S}\left(\vec{U}\right) \tag{4}$$

$$\vec{U}=\begin{bmatrix}\rho\\ \rho u\\ \rho v\\ \rho E\\ \rho S_{xx}\\ \rho S_{yy}\\ \rho S_{xy}\end{bmatrix}\ \vec{E}=\begin{bmatrix}\rho u\\ \rho u^2+p\\ \rho uv\\ u(\rho E+p)\\ \rho S_{xx}u\\ \rho S_{yy}u\\ \rho S_{xy}u\end{bmatrix}\ \vec{F}=\begin{bmatrix}\rho v\\ \rho vu\\ \rho v^2+p\\ \mathrm{v}(\rho E+p)\\ \rho S_{xx}v\\ \rho S_{yy}v\\ \rho S_{xy}v\end{bmatrix}\ \vec{S}=\begin{bmatrix}0\\ \frac{\partial S_{xx}}{\partial x}+\frac{\partial S_{xy}}{\partial y}\\ \frac{\partial S_{xy}}{\partial x}+\frac{\partial S_{yy}}{\partial y}\\ \frac{\partial\left(uS_{xy}+vS_{yy}\right)}{\partial y}+\frac{\partial\left(uS_{xx}+vS_{xy}\right)}{\partial x}+k\nabla^2T\\ 2S_{xy}\Omega_{xy}+2G\bar{D}_{xx}\\ 2S_{xy}\Omega_{yx}+2G\bar{D}_{yy}\\ \Omega_{xy}\left(S_{yy}-S_{xx}\right)+2G\bar{D}_{xy}\end{bmatrix}$$

The kinetics used in the simulation are the same as the slow cook off. In this simulation, level set method and ghost fluid method are used to accurately calculate the behavior of explosives and steel [7]. The governing equations are solved by third-order Runge-Kutta and third-order ENO (essentially non-oscillatory) method with respect to the temporal and spatial discretization respectively. In addition, the time step of hydrocode is determined as

dt = CFL number * dx / (max | sound speed ± local velocity |)(5)

to accurately calculate the governing equations, and the order of time step is approximately 10^{-8}. However, the required calculation time is about 2 minutes based on the experimental results. Thus, at the initial stage of the reaction, the mass and momentum equations are not taken into account but only the energy and species equations are calculated to prevent a lot of computation time. That is why since in the fast cook off situation it reacts thinly on the surface of the explosives, so the effects of pressure and heat generated in the initial stage of the reaction have little impact. At this time, time step is 0.001 seconds. After reaction progress variable is more than 0.1 for PBX # 2, and RDX is all reacted for PBX # 3, thermal runaway occurs. Since then, all governing equations are calculated.

4.2.2 Constitutive relation

Mie-Gruneisen EOS was used for unreacted explosives and gamma-law EOS was used for reaction explosives.

$$p_{unreacted}=\rho_0\Gamma_0 e+\begin{cases}\dfrac{\rho_0c_0^2\varphi}{(1-s\varphi)^2}\left[1-\dfrac{\Gamma_0}{2}\varphi\right] & \text{if } \rho\ge\rho_0\\ c_0^2\left(\rho-\rho_0\right) & \text{otherwise}\end{cases} \tag{6}$$

$$p_{reacted}=\rho RT \tag{7}$$

Johnson-Cook strength model is applied to steel container which is stainless steel 304 [8].

$$\sigma_Y=\left(\sigma_{Y,0}+A\left(\bar{\varepsilon}^P\right)^n\right)\left(1+B\ln\left(\frac{\dot{\bar{\varepsilon}}^P}{\dot{\varepsilon}_0}\right)\right)\left(1-\left(\frac{T-T_0}{T_m-T_0}\right)^m\right) \tag{8}$$

where Γ_0, *s, c₀, A, B, n* and m are material constants, and ρ_0, T_m, T_0, $\bar{\varepsilon}^P$ are initial density, melting temperature, ambient temperature, and effective plastic strain rate, respectively.

	PBX #1 [19]		PBX #2		PBX #3	
	Explosion time (h)	Explosion temperature (°C)	Explosion time (h)	Explosion temperature (°C)	Explosion time (h)	Explosion temperature (°C)
Experiment	~26.02	~173.0	28.98	185.4	21.56	169.4
Simulation	26.88	179.4	29.22	189.0	21.60	164.87

Table 4: Comparison of explosion time and temperature between experiment and simulation

Fast cook off test proceeded according to the procedure of STANAG 4240 [9]. The size of hearth is 1.3m * 0.6m * 0.2m which is sufficient to make the test material engulfed in the fuel-rich flame. The length of explosives is 0.2m and diameter is 0.45m. The density of container is 8000 kg/m^3. Its thermal conductivity is 18.8 W/m·K and the specific heat is 510 J/kg·K [10]. The thickness of casing is 4mm. The computation domain was set based on the actual used test body that is two-dimensional cylinder.

Since the heat penetrated from the flame must be considered in the casing, the following heat transfer is considered at the outermost part. The convective heat flux q_{con} from the flame and the flame to surface radiant flux are defined by

$$q_{con} = h(\mathrm{T}_{flame} - \mathrm{T}) \tag{9}$$

$$q_{rad} = \varepsilon\sigma(\mathrm{T}^4_{flame} - \mathrm{T}^4) \tag{10}$$

where T_{flame} is flame temperature which is obtained as 900℃ on average through the experiment, σ is the Stefan-Boltzmann constant, convective heat transfer coefficient, h is 15 W/m^2·K and surface emissivity, ε is 0.7 [11].

4.2.3 Result

Experiments were conducted twice for only PBX #2 and #3. The reaction progress variable and temperature histories of PBX #2, #3 are plotted in Fig. 4, 5 respectively. The kinetics extracted from DSC for PBX #2 and #3 are found to be appropriate for predicting the explosion times that are 90, 114 seconds in PBX #2, #3 respectively. And explosion temperature is not compared between simulation and experiment since experimental data does not exist.

In setting the kinetics of PBX #3, RDX and AP are set separately. In slow cook off simulation, it was not possible to verify that the kinetics considered to AP are properly extracted by causing explosion as RDX react. While energetic material reacts inside in that circumstance, it reacts thinly on the surface of the explosives under fast cook off condition. And heat of reaction of RDX has much lower than one of AP as shown in the table 2. That is why thermal runaway does not occur only by the reaction of RDX. When AP reacts with relatively high heat of reaction, thermal runaway occurs and reaction occurs violently even though reaction occurs only on the surface. Therefore, it was confirmed that the proposed method of setting the kinetics of PBX #3 was appropriate and this kinetics should be used to accurately predict the explosion time in actual experiments.

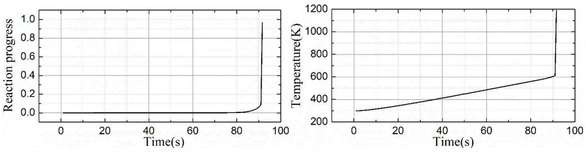

Figure 4: Reaction progress(left) and temperature(right) histories of PBX #2

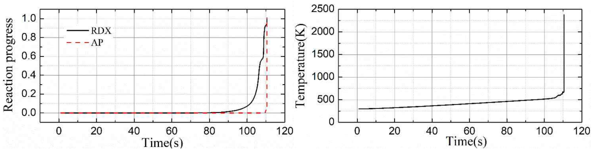

Figure 5: Reaction progress(left) and temperature(right) histories of PBX #3

5 Conclusions

In the current study, when unknown PBX is given, a method for simulating the explosion phenomenon by thermal heating is proposed using kinetics extracted from small amount of PBX sample. The PBXs under study are three types: conventional PBX with HMX of 95%, PBX composed of HMX with 25% of aluminum for afterburning process. Finally, a PBX composed of multi-oxidizer of RDX and AP with aluminum. We have proposed a new methodology to determine the chemical reaction scheme and determine the kinetics for the PBX composed of multi-oxidizer which conventional Friedman analysis cannot be applied. SEM-EDS analysis is additionally performed to verify the assumptions of the chemical reaction model. And the validity of the assumptions is confirmed. We simulate the slow and fast cook off test using extracted kinetics and confirm the validity of the extracted kinetics compared with the experimental results.

6 Acknowledgment

This work was supported by the Agency for Defense Development through IAAT at Seoul National University. And This work was supported by the Brain Korea 21 Plus Project in 2019. Authors are thankful to Dr. J. Park of ADD for conducting the rate stick experiment. Additional funding came from the Advanced Research Center (NRF-2013R1A5A1073861) contracted through the Next Generation Space Propulsion Research Center at Seoul National University.

References

[1] D. Baek, B. Kim, J.J. Yoh, J. Appl. Phys. 124 (21) (2018) 215905.

[2] C. Ping, F. Li, Z. Jian, J. Wei, Propell. Explos. Pyrot. 31 (2006) 452.

[3] S. Vyazovkin, A.K. Burnham, J.M. Criado, L.A. Perez-Maqueda, C. Popescu, N. Sbirrazzuoli, Thermochim. Acta 520 (2011) 1.

[4] T. Boggs, R. Derr, Hazard studies for solid propellant rocket motors (AGARD-AG-316), Advisory Group for Aerospace Research, NATO, 1990.

[5] V. Kodur, M. Dwaikat, R. Fike, J. Mater. Civil Eng. 22 (2010) 423.

[6] J.J. Yoh, M.A. McClelland, J.L. Maienschein, C.M. Tarver, P. Combust. Inst. 31 (2007) 2353.

[7] K. Kim, J. J. Yoh, J. Math. Phys. 49(4), 043511 (2008).

[8] H. Iyama, Y. Higa, M. Nish, S. Itoh, Int. J. Multiphys. 11(3), 233 (2017).

[9] STANAG 4240, Edition 2, “Liquid Fuel / External Fire, Munition Test Procedures,” (2003).

[10] J. N. Sweet, E. P. Roth, M. Moss, Int. J. Thermophys. 8(5), 593 (1987).

[11] M. Graswald, R. Gutser, Proc. Insensitive Munitions Technology Symp. (2018).